Proceedings of ASME Turbo Expo 2024
Turbomachinery Technical Conference and Exposition
GT2024
June 24-28, 2024, London, United Kingdom

GT2024-127941

COMPUTATIONALLY LIGHTWEIGHT METHOD FOR CAMPBELL DIAGRAM PLOTTING IN HIGH-SPEED ELECTRIC MACHINES

Emil Kurvinen[1,*], Qasim Khadim[1], Eero Ikäheimo[1], Tuhin Choudhury[2], Rafal Jastrzebski[3],

[1]University of Oulu, Oulu, Finland
[2]LUT University, Lappeenranta, Finland
[3]University of Turku, Turku, Finland

ABSTRACT

Campbell diagram is plotted from calculation results to identify a rotating object's critical speeds. The Campbell diagram is formed by calculating the supported natural frequencies in a defined operation speed range. It is an important step when designing rotating machines, e.g., an integrated high-speed electric motor that can be sensitive to the rotor's dynamical behavior. Currently, minimizing unnecessary calculation points is important for rapid design iterations and utilization of physics-based models with artificial intelligence. In cases where large variants of rotor geometry or using high-fidelity models, the calculation burden becomes high. In the research, a methodology based on a minimum number of calculation points and a second-order fitting equation is proposed, i.e., instead of using a high number of fixed calculation intervals, a three-point calculation methodology is proposed. The proposed methodology can be applied with neural network-based methods or implemented with high-fidelity models such as solid element models where the physics-based models can be used to create sensitivity to model parameters and study their influence with the traditional rotordynamics Campbell diagram tool. In the results, a comparison of two case studies is shown, and the computational cost is compared.

Keywords: Campbell diagram, Rotordynamics, High-Speed Machines

NOMENCLATURE

Roman letters

a	Polynomial coefficients
$\mathbf{A}$	State matrix
$\mathbf{C}$	Global damping matrix [Ns/m]
F	Fitness function
$\mathbf{F}$	Force vector [N]
$\mathbf{G}$	Global gyroscopic matrix
$\mathbf{I}$	Identity matrix
$\mathbf{K}$	Global stiffness matrix [N/m]
$\mathbf{M}$	Global mass matrix [kg]
t	Time instant [s]
$\mathbf{v}$	Eigenvector
x	Polynomial variable
$\mathbf{x}$	Displacement vector [m]
$\dot{\mathbf{x}}$	Velocity vector [m/s]
$\ddot{\mathbf{x}}$	Acceleration vector [m/s^2]
y	Frequencies [Hz]

Greek letters

α	Real part
β	Imaginary part
λ	Eigenvalue
ω	Rotational speed [rad/s]
ω_i	Damped natural frequencies for i^{th} mode
ζ	Damping ratio for i^{th} mode

Superscripts and subscripts

i	Mode number

1. INTRODUCTION

The Campbell diagram, a frequency-speed diagram, has been widely used when designing rotating machinery to predict resonance frequencies. The methodology was presented a century ago by Wildfred Campbell [1]. In rotating machines, it is important to understand how the rotor which is supported with bearings behaves during operation, and thereby in machines that are performing at the physical limits typically the dynamical behavior becomes important. The resonance frequencies can be shown with the Campbell diagram and, for example, studied with the known excitations (e.g. 1x or its harmonics or subharmonics). [2] In rotating machines, understanding the dynamics is essential when designing new or modifying existing machinery. Electric motor-driven systems, which mostly are rotating electric motors, are consuming 46% of global produced electricity [3]. On the other hand, 96% of electricity is produced with rotating machines

*Corresponding author: emil.kurvinen@oulu.fi

[4]. Timoshenko beam elements are commonly applied when calculating design feasibility in rotordynamics. [5] The Timoshenko beam element can represent well-rotating rotor dynamical behavior in the concept phase. Detailed analyses can be done with more sufficient models such as 3D FEA analysis, e.g. to account for shrink fit opening at high-speed operation [6].

In the control design for example with an Active Magnetic Bearing (AMB) supported rotor the dynamic model is used to design the controller. In the AMBs the position stiffness of the bearing can be varied with the control design [7, 8]. Therefore finding the most suitable combination of bearing stiffness and rotor geometry is required. For further detailed analysis, the vibration amplitudes and changes of eigenfrequencies with the linearized systems are of interest. For nonlinear systems, you typically use phase portraits, and Poincaré maps [9, 10] from simulations. These can give a deeper understanding of the rotating system in the detailed design phase. The computation of e.g. for a high-speed electric machine rotor [11] Timoshenko beam element leads to the matrix that is sized to tens to hundreds in size. With more detailed and complex FEA models the matrix size can be significant and thereby solving one step can take a notable amount of computational capacity [12] for a single rotation speed.

Typically the calculation of Campbell is done at fixed steps, e.g. from 0 rpm to desired rotation speed with fixed incremental size [13]. This leads to unnecessary calculation points and the use of computational capacity [14, 15]. The computational burden of such high-fidelity models can be reduced using the simulation-driven [16] or data-driven [17] surrogates. The surrogate approaches approximate the behavior of a high fidelity model using an approximate model during a time-consuming training phase [16, 17].

The Campbell diagram, as described in [14, 15], appears in linear lines, or, when gyroscopic effects are included, it also takes a nonlinear form that is close to second-order. Therefore, second-order polynomials can be used to describe the Campbell diagram instead of using intensive surrogate training processes. In this study, a method that uses the minimum amount of calculation steps to create a Campbell diagram is proposed. The purpose of minimizing calculation points is to study complex structures' dynamical behavior at the early, conceptual, design stage. The results can be used as indicative for selecting detailed calculation points, where the critical speeds are of interest.

In the study, two different integrated, i.e. the electric machine is in the supported rotor, and high-speed electric machine rotors are used to benchmark the proposed three-point Campbell calculation routine. The first represents a complex case where the frequency order is shifting and frequencies are occurring close to each other and the second is a simple case with frequency order being similar throughout the calculation speed range.

2. METHODS

In the study, a programming platform with custom-built software for rotordynamics is used for calculating the Campbell diagrams. However, the method functions with calculated critical speeds at a given system, e.g. with commercial software.

2.1 Timoshenko beam element

The Finite Element Method (FEM) is used to construct the simulation model for the rotor-bearing system. The rotor shaft is broken down into three-dimensional beam elements along its rotational axis, following Timoshenko's beam theory [18]. Each node of the rotor has four degrees of freedom - two translational and two rotational. The model takes the rotor's geometry and physical parameters as input. The bearing models, made up of spring and damper elements, have their spring stiffness and damping coefficients incorporated into the model at the nodes that represent the actual bearing locations.

2.2 Equation of motion and Cambpell diagram

The equation of motion for a system can be described in general form as,

$$\mathbf{M}\ddot{\mathbf{x}}(t) + (\mathbf{C} + \omega\mathbf{G})\dot{\mathbf{x}}(t) + \mathbf{K}\mathbf{x}(t) = \mathbf{F}(t), \tag{1}$$

where $\mathbf{M}$ is the mass matrix, $\mathbf{C}$ is the damping matrix, ω is the rotational speed, $\mathbf{G}$ is the groscopic matrix and $\mathbf{K}$ is the stiffness matrix of the system. $\mathbf{F}$ is the force vector, which results in $\mathbf{x}$, $\dot{\mathbf{x}}$ and $\ddot{\mathbf{x}}$ representing the displacement, velocity and acceleration vectors, respectively.

Equation (1) can be represented in state-space form by substituting $\mathbf{x}_1 = \mathbf{x}$ and $\mathbf{x}_2 = \dot{\mathbf{x}}$ [19].

$$\begin{cases} \dot{\mathbf{x}}_1 = \dot{\mathbf{x}} = \mathbf{x}_2 \\ \dot{\mathbf{x}}_2 = \ddot{\mathbf{x}} = -\mathbf{M}^{-1}(\mathbf{F}(t) - (\mathbf{C} + \omega\mathbf{G})\mathbf{x}_2 - \mathbf{K}\mathbf{x}_1) \end{cases} \tag{2}$$

Therefore in state space form, equation 1 can be written as:

$$\begin{bmatrix} \dot{\mathbf{x}}_1 \\ \dot{\mathbf{x}}_2 \end{bmatrix} = \begin{bmatrix} \mathbf{0} & \mathbf{I} \\ -\mathbf{M}^{-1}\mathbf{K} & -\mathbf{M}^{-1}(\mathbf{C} + \omega\mathbf{G}) \end{bmatrix} \begin{bmatrix} \mathbf{x}_1 \\ \mathbf{x}_2 \end{bmatrix} + \begin{bmatrix} \mathbf{0} \\ \mathbf{M}^{-1} \end{bmatrix} \mathbf{F}(t) \tag{3}$$

, where $\mathbf{I}$ is the identity matrix.

The state matrix, $\begin{bmatrix} \mathbf{0} & \mathbf{I} \\ -\mathbf{M}^{-1}\mathbf{K} & -\mathbf{M}^{-1}(\mathbf{C} + \omega\mathbf{G}) \end{bmatrix}$, usually denoted by $\mathbf{A}$, can be used to solve the eigen value problem as:

$$\mathbf{A}\mathbf{v} = \lambda\mathbf{v} \tag{4}$$

with $\mathbf{v} \neq 0$, the eigen values will appear in the form of complex conjugate pairs.

$$\lambda_i = \alpha_i \pm j\beta_i \tag{5}$$

where, α_i and β_i represent the real and imaginary parts respectively and $j = \sqrt{-1}$. The damped natural frequencies (ω_i) and the damping ratios (ζ_i) for i^{th} mode can be written as

$$\omega_i = \sqrt{{\alpha_i}^2 + {\beta_i}^2} \tag{6}$$

$$\zeta_i = -\frac{\alpha_i}{\sqrt{\alpha_i^2 + \beta_i^2}} \tag{7}$$

The Campbell diagram can be computed by calculating rotation speed (ω) -dependent values, such as gyroscopic matrix, for each spin speed and then performing an eigenvalue solution for that speed with the equations presented above.

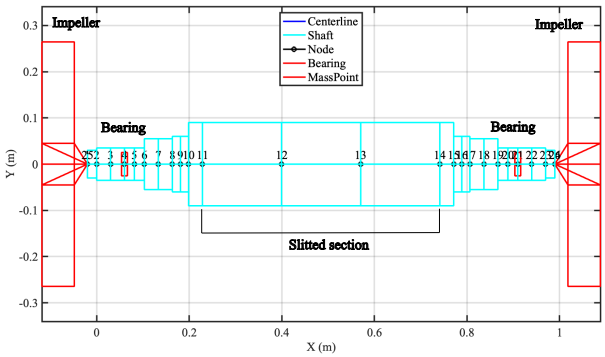

(a) Complex rotor. The slitted part is between nodes 11 and 14.

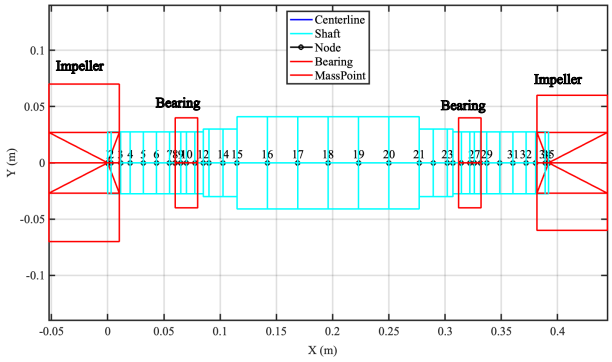

(b) Simple rotor. The impellers are located at nodes 34 and 35.

FIGURE 1: Layout and finite element discretization of the simple and complex rotors with two impellers. The dimensions are in millimeters.

2.3 Fitting algorithm

The typical Campbell diagrams in high-speed electric machines are in the form of straight lines or nonlinearly changing in quadratic form due to the speed and gyroscopic dependent factors.

Due to the simplistic line shapes in the study, a second-order fitting function is used, i.e. $x^2 + x + 1 = 0$. Also due to the low amount of calculation points and complexity in solving the fitting function ordinary least squares (OLS) are used to solve the system of equations $F \cdot a = y$, where F is fitness function, a polynomial coefficient and y solved natural frequencies. The OLS are computationally efficient and give highly accurate solutions. The following workflow is used:

1. Calculate eigenvalues for n speed for x modes
2. Define speed vector for calculated eigenvalues
3. Solve system of equations
4. Visualize the results

3. CASE STUDIES

The proposed calculation methodology is implemented into two different-sized and dynamical behavior rotors. First, *complex rotor*, is a 174.85 kg and 1.010 m long rotor that has a strong gyroscopic effect. The second, *simple rotor*, is 26.00 kg and 0.392 m long, where the gyroscopic effect is not significant. Both rotors are supported with rolling element bearings with constant stiffness. Details of the rotors can be found in earlier studies by Kurvinen et al. [20]. In the results, the colored solid lines represent the reference results from the traditional calculation routine with several calculation points. In this study, the reference speed range for the computation time for calculating the full Campbell diagram in a complex rotor is 33 steps (zero to 16 000 rpm with 500 rpm increments). The results are calculated with the a programming platform with custom build software for rotordynamics in a laptop computer. The computational time with 33 steps is 2.06 seconds, and with the 3-point OLS method 0.34 seconds. For the simple case, it took 3.5 seconds for the full Campbell diagram with 113 steps (zero to 56000 with 500 rpm increment)) and with the 3-point OLS method of 0.5 seconds. It should be noted that the cases represent already simplified Timoshenko beam element-based models. The benefits of the 3-point OLS method come when the model complexity is high, e.g. includes speed-dependent independently solved variables or are high fidelity models.

3.1 a) Complex rotor

The main layout and dimensions of the complex are shown in Fig. 1a while the parameters used in the analysis are shown in Tab. 1.

TABLE 1: Parameters used in the Complex rotor analysis. [20]

Young's modulus	210 GPa
Material density	7800 $\frac{\text{kg}}{\text{m}^3}$
Poisson's ratio (rotor)	0.3
Properties of the slitted part	
Area	0.0251 m^2
Second moment of area	6.2832×10^{-5} m^4
Impeller mass properties	
Mass	19.0 kg
Polar mass moment of inertia	0.5 kg m^2
Diametral mass moment of inertia	0.3 kg m^2
Stiffness of impeller attachment	
Translational	1.0×10^{11} $\frac{\text{N}}{\text{m}}$
Rotational	1.5×10^{6} $\frac{\text{N m}}{\text{rad}}$
Rotor unbalance masses	
D1 Impeller (node 23)	36 g mm @ 270°
D1 Rotor end (node 9)	50 g mm @ 0°
D2 Rotor end (node 14)	50 g mm @ 0°
D2 Impeller (node 24)	50 g mm @ 90°
Total mass of the rotor	174.85 kg

The complex rotor is supported with two 6014/HC2 deep-groove ball bearings (nodes 4 and 19, see Fig. 1a).

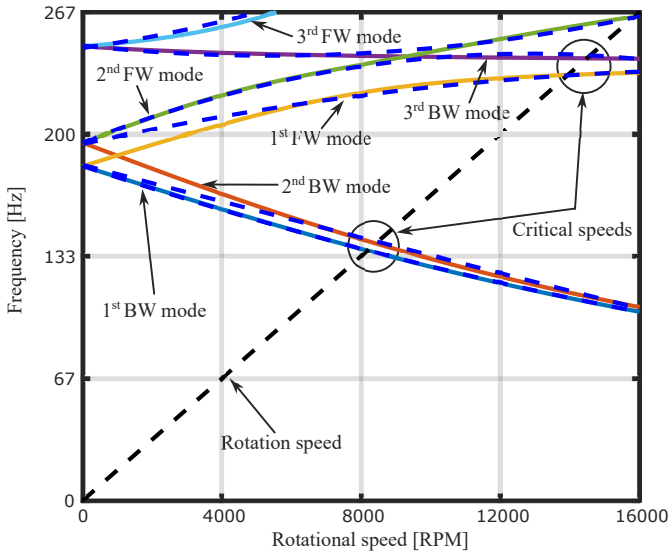

(a) Campbell diagram of the complex rotor

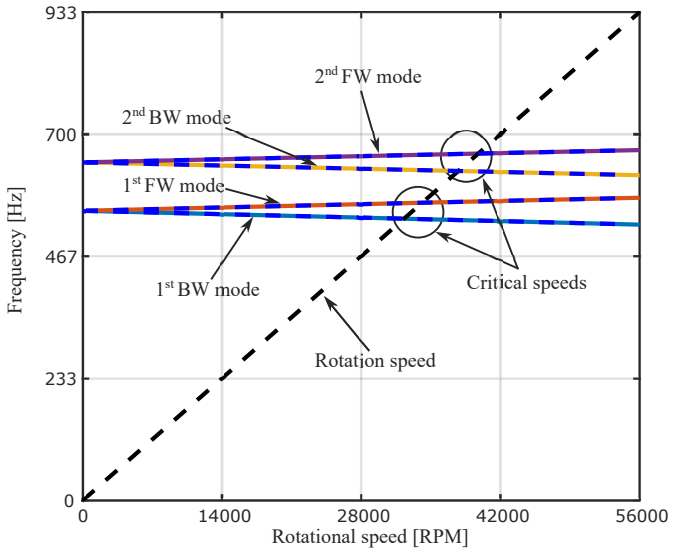

(b) Campbell diagram of the simple rotor

FIGURE 2: Implementation of computationally lightweight method in the simple and complex rotor examples.

3.2 b) Simple rotor

The main layout and dimensions of the simple rotor are shown in Fig. 1b while the parameters used in the analysis are shown in Tab. 2.

TABLE 2: Simple rotor parameters used in analysis [20]

Young's modulus (rotor)	210 GPa
Material density (rotor)	7800 $\frac{kg}{m^3}$
Poisson's ratio (rotor)	0.3
Impeller mass properties	
Mass (node 1)	6.0 kg
Polar mass moment of inertia	0.055 kg m^2
Diametral mass moment of inertia	0.031 kg m^2
Mass (node 35)	5.1 kg
Polar mass moment of inertia	0.028 kg m^2
Diametral mass moment of inertia	0.017 kg m^2
Rotor unbalance masses	
Rotor (node 15 and 21)	0.681 g mm @ 0°
machine (node 1)	0.165 g mm @ 0°
machine (node 35)	0.135 g mm @ 0°
Total mass of the rotor	26.0 kg

The simple rotor is supported with two 71911 CE/HCP4A angular contact ball bearings (nodes 9 and 25, see Fig. 1b)).

3.3 Campbell diagrams

3.3.1 a) Complex rotor. In a Campbell diagram, the natural frequencies of the rotor-bearing systems are shown as a function of rotation speed. The critical speeds are found in the diagram. The Campbell diagram for the complex rotor is shown in Fig. 2a. The dashed blue lines are the results from the proposed calculation algorithm and the colored solid lines from the typical calculation routine (tens of calculation points).

Table 3 shows the complex rotor critical rotation speeds from the Campbell diagram in numerical values and compares the proposed approach results to the benchmarked results

TABLE 3: Complex rotor critical rotation speed from the Campbell diagram FW = Forward whirling, BW = Backward whirling

#	Critical speed rpm		
	Full model	Complex model	Difference [%]
1 (BW)	8, 162	8, 178	−0.20
2 (BW)	8, 269	8, 293	−0.29
1 (FW)	12, 293	12, 414	−0.99
3 (BW)	13, 874	13, 924	−0.36
2 (FW)	15, 219	15, 165	−0.35

Within the studied speed range, five critical speeds occur and are systematically in alignment with the reference results calculated with higher computational burden.

3.3.2 b) Simple rotor. The Campbell diagram simple rotor is shown in Fig. 2b.

Table 4 shows the simple rotor critical rotation speeds from the Campbell diagram in numerical values and compares the proposed approach results to the benchmarked results.

TABLE 4: The critical rotational speed of the simple rotor from the Campbell diagram. FW = Forward whirling, BW = Backward whirling

#	Critical speed rpm		
	Full model	Simple model	Difference [%]
1 (BW)	32, 323.68	32, 323.74	−0.02
1 (FW)	34, 154.85	34, 154.54	0.09
2 (BW)	37, 796.35	37, 796.61	−0.07
2 (FW)	39, 798.30	39, 798.05	0.06

Within the studied speed range four critical speeds occur and are systematically in alignment with the reference results calculated with higher computational burden.

4. DISCUSSION

In the study, the developed algorithm is implemented into two cases and the performance is evaluated. Case a) represents a complex rotor where the different modes cross each other and natural frequencies are close to each other. Case b) represents the case where the natural frequencies do not intersect in speed and critical speeds are behaving linearly. The applications are high-speed electric machine rotors, which have integrated electric machines in these. Both rotors have two impellers, i.e. either two-stage compressors or turbine+compressor possibilities. It should be noted that the methodology requires further development for multistage complex rotor geometries.

The proposed three-point OLS calculation approach to estimating Campbell diagrams yielded good results in the two different complexity cases. For initially estimating the critical speeds the three-point and OLS-based method results in high accuracy with respect to the calculated with full values.

It should be noted that when solving the eigenvalues the order of natural frequencies varies at different speeds thereby tracking the corresponding mode shapes would be beneficial to investigate while computing the natural frequencies. Like in this study, purely the natural frequencies were taken as input in the frequency order. Especially in the complex case, one would assume this to reduce the accuracy, however, the results are very accurate.

The proposed simplified calculation routine enables to exploration of different design variances and finding the design change effect on the critical speeds. With the complex rotor geometries, e.g. including speed and condition loads, such as centrifugal loads and thermal loads the solution time of a single time step can be high.

5. CONCLUSIONS

In the research, the computational efficiency of computing the Campbell diagram in a high-speed electric machine rotor was studied. A three-point calculation routine at zero speed, maximum speed, and middle speed and a second-order fitting were used to estimate critical speeds. For both, very different dynamically behaving cases the critical speed estimation was within one percent accuracy when compared to a typical calculation routine with tens of calculation points. Further investigation into the simplified calculation routine in high-speed electric machine rotors is needed, but the initial results are encouraging.

REFERENCES

[1] Campbell, Wilfred. 1924. *Protection of steam turbine disk wheels from axial vibration*. General Electric Company. DOI 10.1115/1.4058289.

[2] Muszyńska, Agnieszka. 2005. *Rotordynamics*. McGraw-Hill professional engineering, Taylor & Francis, Boca Raton.

[3] Waide, Paul and U. Brunner, Conrad. 2011. "Energy-Efficiency Policy Opportunities for Electric Motor-Driven Systems." IEA Energy Papers 2011/07. Series: IEA Energy Papers Volume: 2011/07.

[4] Ritchie, H. and Rosado, P. 2020. "Electricity Mix." *Our World in Data* .

[5] Shabana, Ahmed A. 2018. *Theory of vibration: an introduction*. Springer.

[6] Sikanen, E., Heikkinen, J.E. and Sopanen, J. 2018. "Shrink-fitted joint behavior using three-dimensional solid finite elements in rotor dynamics with inclusion of stress-stiffening effect." *Advances in Mechanical Engineering* Vol. 10 No. 6 p. 1687814018780054.

[7] Baklouti, A., Dammak, K. and El Hami, A. 2023. "Robust method for the identification of dynamical anisotropic flexible bearing parameters using multi-objective optimization and structural modification technique." *Mechanical Systems and Signal Processing* Vol. 187 p. 109899.

[8] Maslen, E.H., Schweitzer, G., Bleuler, H. and Cole, M. 2009. *Magnetic bearings: theory, design, and application to rotating machinery*. Springer.

[9] Chang, Shun-Chang. 2021. "Study on nonlinear dynamics and chaos suppression of active magnetic bearing systems based on synchronization." *Mathematical Problems in Engineering* Vol. 2021 pp. 1–10.

[10] Ji, L., Chen, K. and Ma, X. 2023. "Mechanism and Mitigation of Actuator Saturation-Induced Vibration in Active Magnetic Bearing-Based Motors." *IEEE Access* .

[11] Choudhury, T., Viitala, R., Kurvinen, E., Viitala, R. and Sopanen, J. 2020. "Unbalance estimation for a large flexible rotor using force and displacement minimization." *Machines* Vol. 8 No. 3 p. 39.

[12] Ao, W., Ke, Z., Zhuo, Z., Zhifeng, X. and Ming, Z. 2023. "Modeling strategy and dynamic analysis of a dual-rotor-bearing-casing system in aero-engine." *Applied Mathematical Modelling* Vol. 123 pp. 105–135.

[13] Shetkar, K.R. and Srinivas, J. 2023. "Vibration analysis and parametric identification of low-pressure steam turbine blade with crack using ANN." *Journal of the Brazilian Society of Mechanical Sciences and Engineering* Vol. 45 No. 6 p. 314.

[14] Saint, M., Leonardo, B., Mendes, R.U. and Cavalca, K.L. 2020. "Model reduction and dynamic matrices extraction from state-space representation applied to rotating machines." *Mechanism and Machine Theory* Vol. 149 p. 103804.

[15] Mogenier, G., Nouri, B.T., Ferraris, G., Dufour, R. and Durantay, L.l. 2012. "A criterion for mode shape tracking: Application to Campbell diagrams." *Journal of Vibration and Control* Vol. 20 .

[16] Khadim, Q., Kurvinen, E., Mikkola, A. and Orzechowski, G. 2023, "Efficient and Accurate Real-Time Simulations of Coupled Mechanical Systems Using the Universal Hydraulic Surrogate." Vol. Volume 10: 19th International Conference on Multibody Systems, Nonlinear Dynamics, and Control (MSNDC): p. V010T10A030.

[17] Bobylev, D., Choudhury, T., Miettinen, J.O., Viitala, R., Kurvinen, E. and Sopanen, J. 2021. "Simulation-Based Transfer Learning for Support Stiffness Identification." *IEEE Access* Vol. 9 pp. 120652–120664.

[18] Nelson, H.D. 1980. "A finite rotating shaft element using Timoshenko beam theory." *J Mech Des* Vol. 102 No. 4 pp. 793–803.

[19] Inman, Daniel J. 2014. *Engineering vibration. Pearson*. Pearson Education.

[20] Kurvinen, E., Sopanen, J. and Mikkola, A. 2015. "Ball bearing model performance on various sized rotors with and without centrifugal and gyroscopic forces." *Mechanism and Machine Theory* Vol. 90 pp. 240–260.

